Optics & Laser Technology 82 (2016) 157–162

Contents lists available at ScienceDirect

Optics & Laser Technology

journal homepage: www.elsevier.com/locate/optlastec

Full length article

Infrared spectral properties for α-$NaYF_4$ single crystal of various Er^{3+}doping concentrations

Cheng Wang [a], Haiping Xia [a,*], Zhigang Feng [a], Zhixiong Zhang [a], Dongsheng Jiang [a], Jian Zhang [a], Shinan He [a], Qingyang Tang [a], Qiguo sheng [a], Xuemei Gu [a], Yuepin Zhang [a], Baojiu Chen [b], Haochuan Jiang [c]

[a] Key laboratory of Photo-electronic Materials, Ningbo University, Ningbo 315211, China
[b] Department of Physics, Dalian Maritime University, Dalian 116026, China
[c] Ningbo Institute of Materials Technology and Engineering, the Chinese Academy of Sciences, Ningbo 315211, China

ARTICLE INFO

Article history:
Received 17 January 2016
Accepted 7 March 2016
Available online 16 March 2016

Keywords:
α-$NaYF_4$ crystals
Er^{3+}
Judd–Ofelt
McCumber theory
Spectral properties

ABSTRACT

The α-$NaYF_4$ single crystals doped with 0.2 mol%, 0.5 mol%, 1 mol%, 2 mol% and 3 mol% Er^{3+} ions were fabricated by an improved Bridgman method. The ~1.5 μm and ~2.7 μm emission properties were investigated in detail through the measured absorption and emission spectra. A Judd–Ofelt analysis of Er^{3+}in α-$NaYF_4$ samples is performed. The Judd–Ofelt parameters are obtained ($\Omega_2 = 2.71 \times 10^{-20}$ cm^2, $\Omega_4 = 2.28 \times 10^{-20}$ cm^2, $\Omega_6 = 0.84 \times 10^{-20}$ cm^2) and the radiative lifetimes of Er^{3+}energy levels and the branching ratios of Er^{3+}transitions are calculated. The calculated maximum emission cross section by McCumber theory for ~1.5 μm and ~2.7 μm reached 1.35×10^{-20} cm^2 and 2.2×10^{-20} cm^2, respectively. The gain cross section spectra were calculated based on the absorption and emission cross section spectra. All these spectral properties indicated that this kind of fluoride crystal has potential application as host material for infrared lasers.

1. Introduction

In recent decades, the infrared solid state lasers have attracted much attention because of their many applications including environment monitoring, laser processing, distance measurement, military and many other fields [1–3]. It is noted that rare-earth ions in the low phonon energy of the host material in the infrared multi-phonon relaxation transition rate is greatly reduced, so that the infrared radiation transitions become possible [4]. Erbium ion (Er^{3+}) is one of the most important rare earth ions due to the efficient emission band from UV to mid-infrared. Up to know, a lot of Er^{3+}doped crystals such as Er^{3+}:$Y_3Al_5O_{12}$ [5], Er^{3+}:$Ca_9Y(VO_4)_7$ [6], Er^{3+}:$La_3Ga_{5.5}Ta_{0.5}O_{14}$ [7], Er^{3+}:$LiNbO_3$ [8] and Er^{3+}:$LiYF_4$ [9] have shown efficient spectral properties, and the lasers at about ~1.5 μm via $^4I_{13/2} \rightarrow {}^4I_{15/2}$ have been outputted successfully from activator Er^{3+}based solid materials [10–14]. Recently, the development of mid-infrared laser at ~2.7 μm via $^4I_{11/2} \rightarrow {}^4I_{13/2}$ transitions of Er^{3+}doped solid materials becomes considerable interest because of their special application in military and environment monitoring.

It is well known that the luminescence of Er^{3+}in traditional oxide crystals tend to be quenched easily by the rapid multi-phonon effect due to their high phonon energies. Furthermore, in order to obtain high luminescent efficiency at ~2.7 μm, matrix with low phonon energy should be chosen because of the narrow energy difference between $^4I_{11/2}$ and $^4I_{13/2}$ levels. Thus it becomes vital and important to explore new host materials with low phonon energies.

The cubic α-$NaYF_4$ has been widely studied because of its low maximum phonon energy and the applications of these crystals as excellent hosts for up-conversion [15]. More recently, the α-$NaYF_4$ single crystals doped with Ho^{3+}/Yb^{3+}[16], and Tm^{3+} [17] were successfully grown in our laboratory by an improved flux-Bridgman method. The transmittance in the range of infrared and mid-infrared, and Raman spectra of α-$NaYF_4$ single crystal have been already recorded in our laboratory [18]. It shows high transmittance in range of infrared and mid-infrared and the maximum phonon energy of α-$NaYF_4$ single crystal about 390 cm^{-1}. Compared with $LiYF_4$ single crystal [9], the α-$NaYF_4$ shows further lower phonon energy and higher transparency in range of infrared and mid-infrared [16,17]. The excellent properties of α-$NaYF_4$ single crystal in optical behaviors and physical-chemical properties are beneficial for infrared and mid-infrared laser application to obtain high luminous efficiency and high stability. However, there are few reports about Er^{3+}ion doped α-$NaYF_4$ for infrared and mid-infrared laser because of the difficulty of the crystal growth.

In this paper, α-$NaYF_4$ samples with different Er^{3+}doping

---

* Corresponding author.
E-mail address: hpxcm@nbu.edu.cn (H. Xia).

http://dx.doi.org/10.1016/j.optlastec.2016.03.012
0030-3992/© 2016 Elsevier Ltd. All rights reserved.

concentrations (0.2, 0.5, 1, 2, 3 mol%) were grown successfully by an improved Bridgman method using KF as flux. The absorption spectrum was detected and the optical parameters were calculated. The emission spectrum of ~1.5 μm and ~2.7 μm for Er^{3+}singly doped α-$NaYF_4$ crystal were investigated. It is expected that this study provides a good theoretical basis for the further development and implementation of infrared devices.

2. Experimental

The Er^{3+}doped α-$NaYF_4$ single crystals in 10 mm diameter investigated in our study were fabricated by the Bridgman method with molar compositions of 30NaF-18KF-(52-χ)YF_3-χErF_3 (χ=0.2, 0.5, 1.0, 2.0, 3.0). The mixtures were treated by fluoridated method with anhydrous HF at 750–800 °C for 8–10 h to remove the influence of the hydroxyl ion OH^- concentration in these crystals. A low OH^- content is important in order to eliminate the non-radiative energy transfer from the excited level of Er^{3+} ion to OH^-. The specific details and processes of crystal growth were described in Ref. [19].

The polished slices of various concentrations are shown in the inset of Fig. 1(a).The X-ray diffraction patterns of samples were recorded with a XD-98X diffractometer (XD-3, Beijing). The concentration of Er^{3+}in this sample was measured with inductively coupled plasma atomic emission spectrum (ICP-AES, PerkinElmer Inc., Optima 3000). The absorption spectrum was detected by a Cary 5000 UV/VIS/NIR spectrophotometer in the wavelength region from 200 nm to 2200 nm. The emissions spectra were investigated with a Traix 320 type spectrometer in the range of 1000–1800 nm, and 2500–3000 nm excited by 980 nm light. All measurements were carried out at room temperature. A FLSP 920 type spectrometer (Edinburgh Co., England) excited by 980 nm LD was used to obtain the fluorescence lifetime.

3. Results and discussion

3.1. X-ray diffraction

Although we have obtained α-$NaYF_4$ crystals with different doping concentrations of Er^{3+}, the higher doping level has a greater impact on the structure of crystal, and the XRD diffraction pattern of the sample with 3 mol% is plotted in Fig. 1(b). By comparing with the JCPDS card of α-$NaYF_4$ (No.77-2042) of cubic system [16–18] illustrated in Fig. 1(c), it can be seen that the current doping level does not cause any obvious peak shift or another phase, indicating that this transparent crystal has pure cubic phase and Er^{3+} ions perfectly entered the Y^{3+}sites. The calculated cell parameters from the XRD pattern for Er^{3+}singly doped α-$NaYF_4$ crystal are a=b=c=0.5514 nm. As labeled in Fig. 1, the lattice parameters of the Er^{3+}doped one are a bit larger than the blank matrix, it is well in agreement with the fact that the radius of $Er^{3+}$is greater than Y^{3+}.

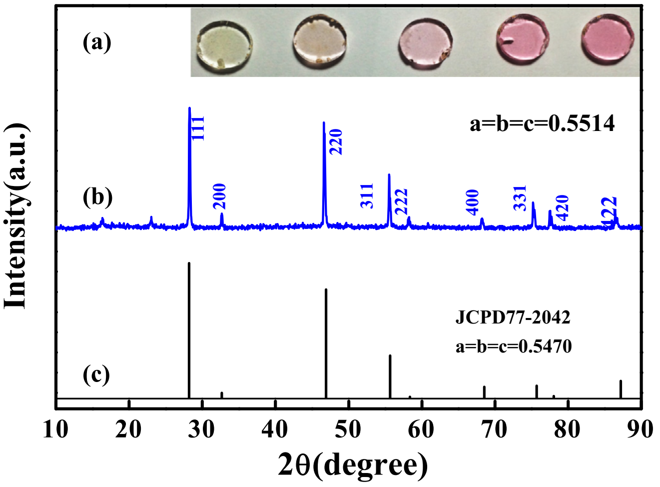

Fig. 1. (a) XRD curve of Er^{3+}singly-doped α-$NaYF_4$ crystal with molar concentration of 3 mol%. (b) The standard line pattern of α-$NaFY_4$ (JCPDS 77-2042).

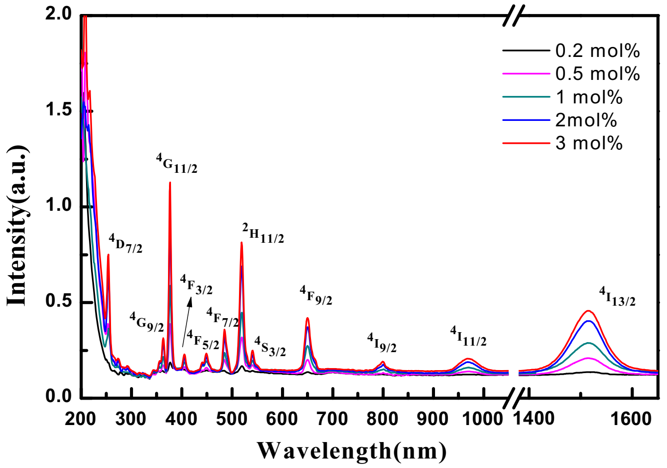

Fig. 2. Absorption spectra of various concentrations of Er^{3+}doped α-$NaYF_4$ single crystals.

3.2. Absorption spectra and Judd–Ofelt analysis

Fig. 2 presents the absorption spectra of α-$NaYF_4$ samples with different erbium doping concentrations in the wavelength region of 200–1050 nm and 1400–1650 nm at room temperature. The absorption bands at 377, 487, 517, 650, 792, 980, 1517 and 2700 nm of Er^{3+}, which are closely related to the transitions from the ground state $^4I_{15/2}$ to $^4G_{11/2}$, $^4F_{7/2}$, $^2H_{11/2}$, $^4F_{9/2}$, $^4I_{9/2}$, $^4I_{11/2}$ and $^4I_{13/2}$ excited states. It can be seen from Fig. 2 that the absorption intensity gradually increases as the doping concentration changes from 0.2 to 3 mol%, and there are no miscellaneous peaks appearing or any peak shifts. A broad absorption peak concentrated at 980 nm indicates that Er^{3+}ion can act as an excellent activator to absorb the 980 nm pump light. Therefore, the excellent infrared transmission property provides potential application for mid-infrared laser material.

Judd–Ofelt (J–O) theory [20,21] is extensively used in the analysis of spectroscopic characters of rare earth elements in laser materials. Based on J–O theory, the absorption spectra can be used to calculate the oscillator strength parameter Ω_t (t=2, 4, 6), radiative lifetime τ_{rad}, fluorescence branching ration β and transition probability A. To the best of our knowledge, there are rarely Judd–Ofelt analyses of Er^{3+}in hosts isomorphous with α-$NaYF_4$ published in the literature. In this work, the J-O intensity parameters of Er^{3+}doped α-$NaYF_4$ were calculated.

According to the absorption spectrum, the experimental oscillator strengths are obtained by the following expression [22]:

$$f_{\exp} = \frac{mc^2}{\pi e^2 N}\int \frac{2.303OD(\lambda)}{\lambda^2 d} d\lambda \qquad (1)$$

where m is the electron mass, e is the electron charge, N is the number of the absorbing ions in unit volume, $OD(\lambda)$ is the optical density, c is the speed of light and d is the thickness of the sample.

According to Judd–Ofelt theory, the calculated oscillator strengths are obtained by the following expression: